CYBERNETICS AND PHYSICS, VOL. 6, NO. 3, 2017 , 131–138

CUSP CATASTROPHE IN A BISTABLE PERCEPTION ENERGY MODEL WITH ADDITIVE AND PARAMETRIC NOISE

Irina Bashkirtseva
Institute of Natural Science
and Mathematics
Ural Federal University
Ekaterinburg, Russia
irina.bashkirtseva@urfu.ru

Lev Ryashko
Institute of Natural Science
and Mathematics
Ural Federal University
Ekaterinburg, Russia
lev.ryashko@urfu.ru

Alexander N. Pisarchik
Center for Biomedical Technology
Technical University of Madrid
Madrid, Spain
alexander.pisarchik@ctb.upm.es

Abstract

Using the cusp catastrophe theory formalism we analyze stochastic sensitivity of a bistable energy model, often used for description of visual perception, subject to both additive and parametric noise. In perception psychology, different kinds of noise may be associated with inherent brain noise originated from physiological processes and random synaptic connections of brain neurons due to interactions among neural networks. We demonstrate that parametric noise leads to the total suppression of oscillations when the system stays in an unstable equilibrium, whereas in the presence of additive noise the oscillations still exist, but strongly suppressed. Using a new approach based on the stochastic sensitivity function and the method of confidence intervals we demonstrate the effect of noise on the range of hysteresis observed in bistable perception when a control parameter is changed. This approach allows prediction of the hysteresis squeezing when the intensity of additive noise is increased. Stochastic bifurcations associated with transformation of the system from bistable to monostable are studied using probability density functions.

Key words

Perception model, bistability, hysteresis, noise.

1 Introduction

Some authors emphasized that perception of ambiguous images can be modeled by using the catastrophe theory formalism [Poston and Stewart, 1978; Ta'eed, Ta'eed and Wright, 1988]. Catastrophe theory, as a branch of bifurcation theory, studies sudden dramatic changes in the behavior of dynamical systems arising when various control factors are varied. Originated by the French mathematician René Thom in the 1960s, the catastrophe theory became very popular in the 1970s due to efforts of Christopher Zeeman, who applied this theory to a number of different phenomena observed in biological and behavioral systems [Zeeman, 1977; Saunders, 1980]. Phenomenologically, a type of catastrophe is determined by a number of parameters simultaneously varied. Nowadays, one can distinguish up to nine fundamental types of catastrophe. The most common ones are fold, cusp, swallowtail, and butterfly.

At the beginning of its creation, the catastrophe theory was not applicable for description of cognitive experiments, because catastrophe models were developed to describe deterministic systems only, whereas psychology and cognitive sciences dealt with stochastic systems. However later stochastic formulations of catastrophe theory allowed quantitative comparison of catastrophe models with experimental data [Cobb and Ragade, 1978; Cobb and Watson, 1980; Cobb, 1981; Ploeger et al, 2002; Grasman et al, 2009], including visual perception [Stewart and Peregoy, 1983; Fürstenau, 2006].

In the last two decades, noise-induced non-equilibrium phenomena have attracted a great deal of attention due to various interesting effects produced by noise. For instance, it was found that small noise underlies various probabilistic phenomena, such as noise-induced transitions [Horsthemke and Lefever, 1984; Moss and McClintock, 1989; Anishchenko et al, 2007], stochastic resonance [Pikovsky and Kurths, 1997; Gammaitoni et al, 1989; McDonnell et al, 2008], noise-induced order-chaos transformations [Matsumoto and Tsuda, 1983; Gassmann, 1997; Gao, Hwang, and Liu, 1999; Lai and Tel, 2011], and noise-induced intermittency [Lai and Grebogi, 1995; Pisarchik et al, 2012; Grubov et al, 2017]. Different effects of additive and parametric noise have also been demonstrated using the bistable van der Pol oscillator and the Hopf system with coexisting fixed point and limit cycle [Bashkirtseva, Ryashko and Schurz, 2009; Bashkirtseva, Ryazanova, and Ryashko, 2015].

In this paper, we analyze a stochastic energy model often used for description of visual perception of ambiguous images. Using a cusp catastrophe theory formalism, we study, for the first time to our knowledge, the influence of both additive and parametric noise on the stability of this system. The different types of noise may be associated, respectively, with inherent brain noise originated from physiological processes and random synaptic connections of brain neurons. The latter arises as a consequence of interactions among different parts of brain neural networks functioning in a coordinated fashion, with associated energy exchange. Since cognition involves different classes of long range correlated processes among brain regions supported at the neuronal level, it results in distinct manifestations of cerebral activity. We estimate the hysteresis value in the bistable perception model using an analytical approach based on the stochastic sensitivity functions technique and the method of confidence intervals.

2 Deterministic Perception Model

Let us consider the simple double-well potential deterministic model used for description of bistable perception [Moreno-Bote, Rinzel, and Rubin, 2007; Huguet, Rinzel, and Hupé, 2014; Pisarchik et al, 2014; Pisarchik, Bashkirtseva, and Ryashko, 2015]:

$$\dot{x} = -4ax(x^2 - b) + 4c, \tag{1}$$

where x is a cognition variable, c is a metabolic activity parameter, a is an ambiguous parameter, and b is a synaptic overlap parameter. The parameter b reflects a probabilistic character of the synaptic overlap of distinct brain areas responsible for visual perception. Cognition is directly related to both metabolic activity and synaptic connectivity. All these processes are associated with neuronal connectivity. An increase in connectivity enlarges the neural network involved into cognitive processes, thus stimulating metabolic activity. A lack of metabolic activity unrelated to cognitive demands (and network connectivity) due to some reasons, e.g. Alzheimer disease, results in degradation of existing neural networks.

The model Eq. (1) exhibits the coexistence of two fixed points in the double-well potential $U = a(x^4 - 2bx^2) - 4cx$ shown in Fig. 1 for two different values of c. The parameters a and b describe respectively a depth of the potential wells and a distance between these wells. When the parameter b changes its sign from minus to plus, the potential transforms its shape from one-well to two-well. In what follows, we set

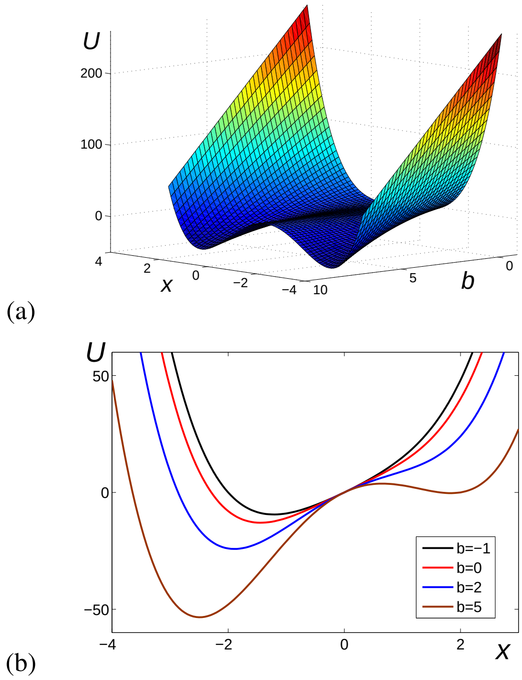

Figure 1. Potential $U = x^4 - 2bx^2 - 4cx$ as a function of x and b for (a) $c = 0$ and (b) $c = -3$.

$a = 1$, while both b and c are used as control parameters.

The deterministic system Eq. (1) for $b > 0$ has two bifurcation borders:

$$c_1(b) = -\frac{2\sqrt{3}}{9}\, b^{3/2}, \; c_2(b) = \frac{2\sqrt{3}}{9}\, b^{3/2}.$$

For $c < c_1$, the system exhibits a single stable equilibrium $\bar{x}_1(b, c)$. In a zone $c_1 < c < c_2$, after passing saddle-node bifurcation point c_1, the system has two stable equilibria, $\bar{x}_1(b, c)$ and $\bar{x}_3(b, c)$, separated by the unstable equilibrium $\bar{x}_2(b, c)$. For $c > c_2$, the system exhibits a single stable equilibrium $\bar{x}_3(b, c)$.

For $b \leq 0$, the deterministic system Eq. (1) has a single stable equilibrium $\bar{x}(b, c)$.

Stable equilibria $\bar{x}$ of the deterministic system Eq. (1) are plotted in Fig. 2 in the (b, c, x) space. One can see that this deterministic model exhibits a well-known cusp catastrophe.

The projections of the attractors to different fixed values of b are shown in Fig. 3. The cusp model describes hysteresis which takes place for $b > 0$ when c is gradually increased and decreased.

As can be seen in Figs. 2 and 3, hysteresis is accompanied by a divergence caused by increasing the splitting parameter b. Hysteresis only exists when b is relatively high. Both divergence and hysteresis also depend on the parameter c.

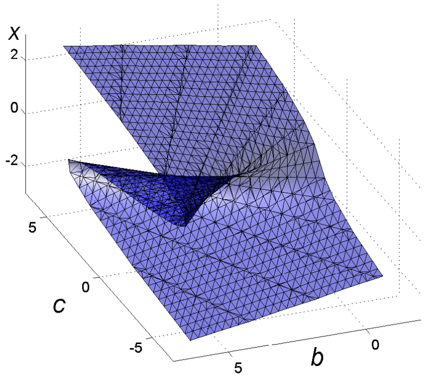

Figure 2. Attractors of system $\dot{x} = -4x(x^2 - b) + 4c$.

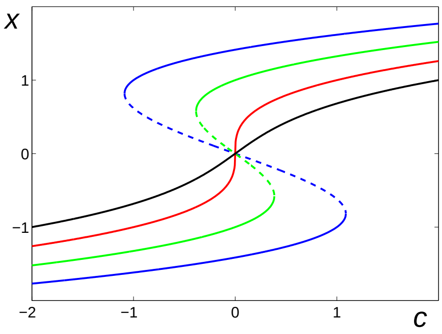

Figure 3. Stable (solid) and unstable (dashed) equilibria of deterministic model $\dot{x} = -4x(x^2 - b) + 4c$ for $b = -1$ (black), $b = 0$ (red), $b = 1$ (green), and $b = 2$ (blue).

3 Stochastic System

Let us now consider the stochastic model in Ito's sense:

$$\dot{x} = -4ax\left[x^2 - (b + \varepsilon\xi_1(t))\right] + 4c + \varepsilon_{add}\xi_2(t), \quad (2)$$

where ε is an intensity of parametric noise acting on the parameter b, and ε_{add} is an intensity of additive noise. In Eq. (2) $\xi_{1,2}(t)$ are uncorrelated white Gaussian noises with parameters $\mathrm{E}\xi_i(t) = 0, \quad \mathrm{E}(\xi_i(t)\xi_j(\tau)) = \delta(t-\tau)\delta_{ij}, \quad i,j = 1,2$.

Figure 4 shows the time series of the system in Eq. (2) forced by parametric noise only for the parameters inside the bistability zone. One can see that when the noise intensity is increased, the amplitudes of separated coexisting oscillations also increase and mix, leading to stabilization of an unstable equilibrium. Such noise-induced suppression of oscillations is explained by singularity of parametric noise that vanishes at $x = 0$. Thus, strong parametric noise in this system stabilizes the unstable equilibrium and annihilates hysteresis.

The effect of small additive noise $\varepsilon_{add} = 0.01$ is illustrated with the time series in Fig. 5, for the same parameters as in Fig. 4. Although the oscillations are highly suppressed by the very strong parametric noise ($\varepsilon = 1$), they still exist near the unstable equilibrium $x = 0$ with small amplitude. [Fig. 5(d)].

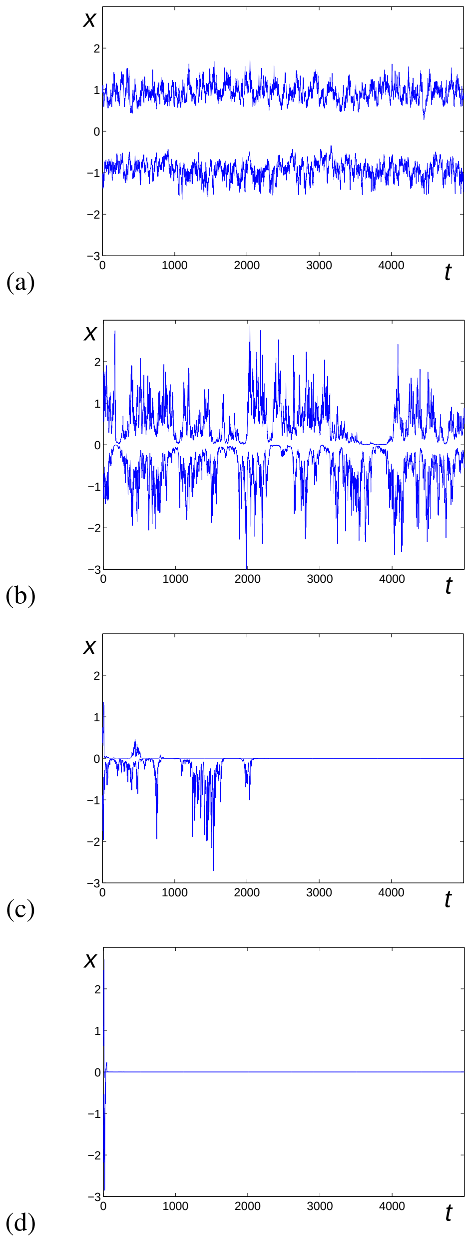

Figure 4. Time series for stochastic model in bistability zone with parametric noise only (without additive noise, i.e. $\varepsilon_{add} = 0$) and $b = 1$, $c = 0$: (a) $\varepsilon = 0.2$, (b) $\varepsilon = 0.5$, (c) $\varepsilon = 0.7$, and (d) $\varepsilon = 1$.

Interestingly, even in monostability zones stochastic trajectories nestle to $x = 0$ under parametric noise, despite in this point there is no any equilibrium. This effect is observed without additive noise (Fig. 6) and with it (Fig. 7).

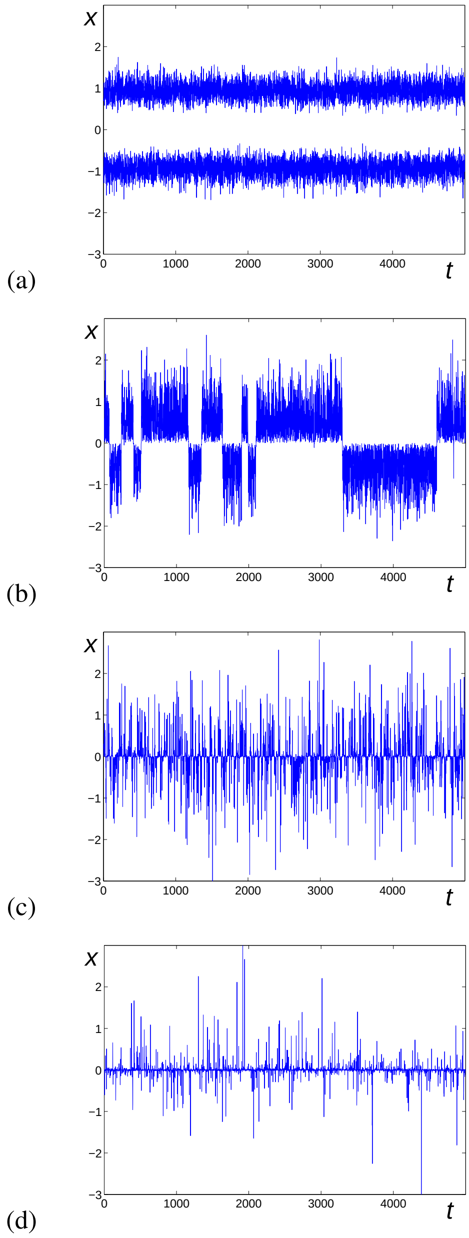

Figure 5. Time series for stochastic model in bistability zone with both parametric and additive noise for $b = 1$, $c = 0$, $\varepsilon_{add} = 0.01$ and (a) $\varepsilon = 0.2$, (b) $\varepsilon = 0.5$, (c) $\varepsilon = 0.7$, (d) $\varepsilon = 1$.

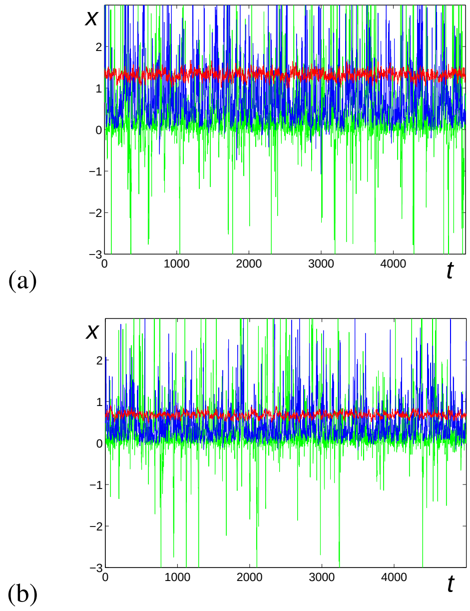

Figure 6. Time series for stochastic model Eq. (2) in monostability zone without additive noise ($\varepsilon_{add} = 0$) for $c = 1$, $\varepsilon = 0.1$ (red), $\varepsilon = 1$ (blue), $\varepsilon = 2$ (green) for (a) $b = 1$ (starting from upper equilibrium) and (b) $b = -1$.

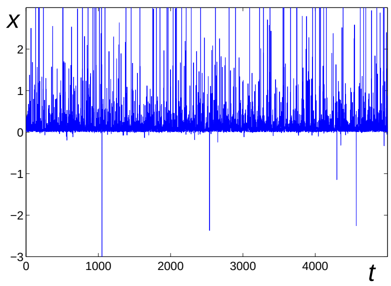

Figure 7. Time series for stochastic model in monostability zone with additive noise ($\varepsilon_{add} = 0.01$) with $b = 1$, $c = 1$, and $\varepsilon = 3$.

3.1 Stochastic Sensitivity Analysis

In order to analyze the influence of noises on the hysteresis, we use the stochastic sensitivity function (SSF) technique and the method of confidence intervals introduced in [Bashkirtseva and Ryashko, 2011; Bashkirtseva, Neiman, and Ryashko, 2013] (for short background see Appendix).

For the system in Eq. (2) without additive noise, for $b > 0$, stochastic sensitivity functions $M_1(b, c)$ and $M_3(b, c)$ of equilibria $\bar{x}_1(b, c)$ and $\bar{x}_3(b, c)$ are

$$M_1(b, c) = \frac{2a^2\bar{x}_1^2(b, c)}{3\bar{x}_1^2(b, c) - b} \quad \text{for } c < c_2,$$

$$M_3(b, c) = \frac{2a^2\bar{x}_3^2(b, c)}{3\bar{x}_3^2(b, c) - b} \quad \text{for } c > c_1.$$

For $b < 0$, the stochastic sensitivity function $M(b, c)$

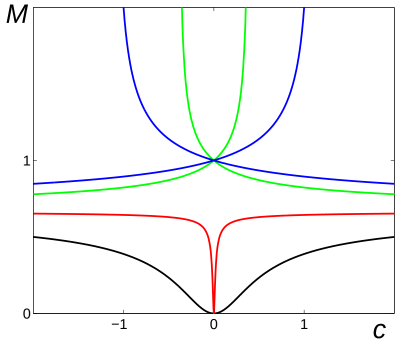

Figure 8. Stochastic sensitivity of stable equilibria of system Eq. (2) with $\varepsilon_{add} = 0$ and $b = -1$ (black), $b = -0.1$ (red), $b = 1$ (green), and $b = 2$ (blue).

of the single stable equilibrium $\bar{x}(b, c)$ is

$$M(b, c) = \frac{2a^2\bar{x}^2(b, c)}{3\bar{x}^2(b, c) - b}.$$

Figure 8 shows plots of the stochastic sensitivity functions $M_1(b, c)$, $M_3(b, c)$, for $b > 0$, and $M(b, c)$ for $b < 0$, versus the parameter c for the system in Eq. (2) without additive noise. These functions are symmetric with respect to $c = 0$. As one can see, the stochastic sensitivity $M(b, c)$ of the equilibrium $\bar{x}$ is bounded whereas the stochastic sensitivity $M_{1,3}(b, c)$ of the equilibria $\bar{x}_{1,3}$ unlimitedly grows as the parameter c approaches $c_{1,2}$. For $b = 0$, the stochastic sensitivity is independent of c.

In Fig. 9 we plot the random states (green) and inner borders (red) of confidence intervals found by the SSF technique. In the stochastic system, the hysteresis value can be estimated as the distance between the red lines in section $x = 0$. The confidence intervals (red lines) indicate squeezing of the hysteresis range as parametric noise is increased.

4 Stationary Probabilistic Density: Stochastic Merging Bifurcation

The analytic description of the solutions of Eq. (2) is given by the stationary density distribution $\rho(x)$. For small noises, the density has peaks near stable equilibria and wells near an unstable equilibrium. Therefore, in the bistability zone, the function $\rho(x)$ has two maxima, whereas in the monostability zone only one. A change in the additive noise intensity has no influence on the number and position of the maxima. When the parametric noise intensity is increased, the two well separated maxima approach each other and merge. Thus, the bistable system can be converted into a monostable. Such transformation is a key point in understanding probabilistic mechanisms of the changes

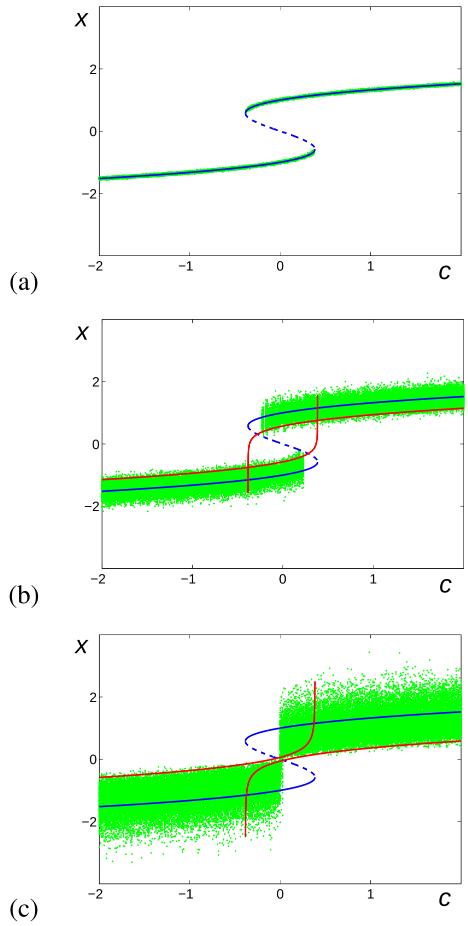

Figure 9. Random states (green) and equilibria (blue) of system Eq. (2) with $b = 1$ and $\varepsilon_{add} = 0$ for (a) $\varepsilon = 0.02$, (b) $\varepsilon = 0.2$, and (c) $\varepsilon = 0.5$. In the panels (b) and (c) the inner boundaries of the confidence intervals are plotted in red.

in perception under the influence of noise. The noise-induced transition from bistability to monostability is also of general interest for controlling multistability [Pisarchik, Bashkirtseva, and Ryashko, 2015; Sevilla-Escoboza et al, 2015].

The parametric description of the stochastic merging bifurcation which separates the monostable and bistable regions is illustrated in Fig. 10. The blue curve defined by the functions $c_{1,2}(b)$ shows the bifurcation boundary for the deterministic system Eq. (2). In the left-hand side from the line the system is monostable, whereas in the right-hand side it is bistable. For the stochastic system, the bifurcation boundary (red line) is given by the following equation

$$c(b, \varepsilon) = \pm\frac{2\sqrt{3}}{9}\left(b - 4\varepsilon^2\right)^{3/2},$$

where ε is the intensity of parametric noise. One can see that parametric noise shifts the boundary to the

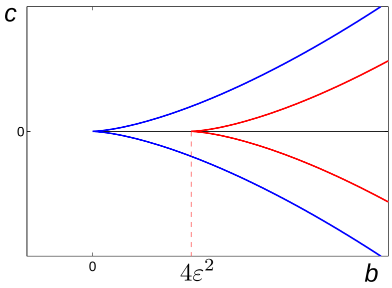

Figure 10. Zones of monostability and bistability for deterministic system (blue line) and with parametric noise (red line).

right side (red line), thus enlarging the monostability zone.

From the above analysis, it follows that there is a critical value of the parametric noise intensity $\varepsilon^* = \frac{1}{2}\sqrt{b - \frac{3}{\sqrt[3]{4}}c^{2/3}}$ needed to transform the bistable system to monostable.

The probability distribution function of x values provides with significant information about the noise-induced transition from bistability to monostability. In Fig. 11 we plot the extrema of stationary density distribution versus the parametric noise intensity ε for $c = 0$ [Fig. 11(a)] and $c > 0$ [Fig. 11(b)].

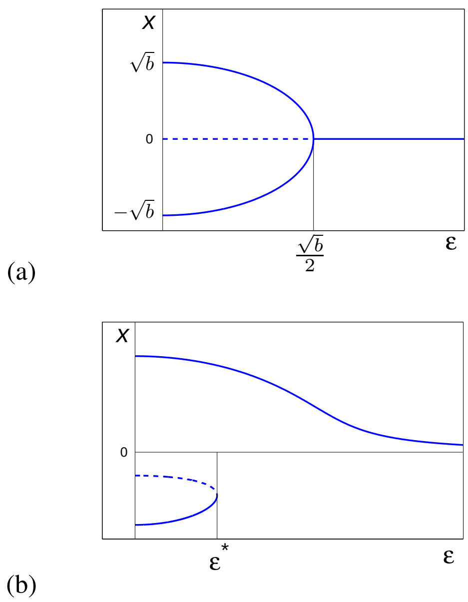

Figure 11. Extrema of probability distribution function of x at (a) $c = 0$ and (b) $c > 0$. The maxima and minima are plotted by the solid and dashed lines, respectively.

One can see that the peaks merge only in the case of symmetry when $c = 0$. Here, the critical noise intensity is $\varepsilon^* = \sqrt{b}/2$. For $\varepsilon > \varepsilon^*$ the maximum density is located exactly above $x = 0$. For $c > 0$, the transition from bimodality to unimodality is different. When the parametric noise intensity is increased, one of the peaks disappears, one of the maxima merges with the minimum, and another maximum approaches $x = 0$ only asymptotically.

5 Conclusion

Using catastrophe theory formalism we have analyzed a stochastic model for visual perception under the influence of additive and parametric noise. Even though the model is very simple, it models several known facts about cognitive decline and dementia. The system is derived solely from the application of the law of conservation of energy and its behavior does not require other mechanistic explanations. In this formulation, dementia is irreversible, not because of the destruction of the physical network, but because of the involved energy and the loss of synaptic overlap. This implies that neurons can still be functional, but if the degree of linkage between them is not sufficient, then the cognitive network behaves as if the neurons were lost.

For the conceptual model under consideration, peculiarities of the impact of additive and parametric noises have been studied and discussed. Without additive noise, an increase in the parametric noise intensity resulted in the disappearance of oscillations, where the system stabilized in an unstable equilibrium, whereas in the presence of additive noise the oscillations are strongly suppressed but do not disappear. In the stochastic energy model, the hysteresis range provides with significant information about perception mechanisms. In order to study the influence of noise on the hysteresis, we used an analytical approach based on the stochastic sensitivity functions technique, and the method of confidence intervals. The mutual arrangement of the confidence intervals borders allowed us to estimate the hysteresis value. We have shown that an increase in the noise intensity resulted in a decrease in the distance between these borders and specified the hysteresis squeezing. Qualitative changes of the stationary probabilistic density (stochastic bifurcations) connected with the transformation of the system from bistable to monostable have been investigated, and the detailed parametric description of such stochastic bifurcations has been given.

Acknowledgements

The development of a mathematical model for perception and the analysis of its deterministic properties were carried out by A.N.P and supported by the Ministry of Economy and Competitiveness (Spain) (project SAF2016-80240). The stochastic analysis was carried out by I.B. and L.R. and supported by the Russian Science Foundation (project 16-11-10098).

References

Anishchenko, V.S., Astakhov, V.V., Neiman, A.B., Vadivasova, T. E., and Schimansky-Geier, L. (2007). *Nonlinear Dynamics of Chaotic and Stochastic Systems: Tutorial and Modern Development*. Springer-Verlag. Berlin-Heidelberg.

Bashkirtseva, I., Ryashko, L., and Schurz, H. (2009). Analysis of noise-induced transitions for Hopf system with additive and multiplicative random disturbances. *Chaos, Solitons and Fractals*, **39**, pp. 72–82.

Bashkirtseva, I., Neiman, A.B., and Ryashko, L. (2013). Stochastic sensitivity analysis of the noise-induced excitability in a model of a hair bundle. *Phys. Rev. E*, **87**, p. 052711.

Bashkirtseva, I., Ryazanova, T., and Ryashko, L. (2015). Stochastic bifurcations caused by multiplicative noise in systems with hard excitement of auto-oscillations. *Phys. Rev. E*, **92**, p. 042908.

Bashkirtseva, I. and Ryashko, L. (2011). Sensitivity analysis of stochastic attractors and noise-induced transitions for population model with Allee effect. *Chaos*, **21**, p. 047514.

Cobb, L. and Ragade, R.K. (1978). Applications of catastrophe theory in the behavioral and life sciences. *Behavioral Science*, **23**, pp. 291–298.

Cobb, L. and Watson, B. (1980). Statistical catastrophe theory: An overview. *Mathematical Modelling*, **1**, pp. 311–317.

Cobb, L. (1981). Parameter estimation for the cusp catastrophe model. *Behavioral Science*, **26**, pp. 75–78.

Fürstenau, N. (2006). Modelling and simulation of spontaneous perception switching with ambiguous visual stimuli in augmented vision systems. *Perception and Interactive Technologies*, **4021**, pp. 20–31.

Gammaitoni, L., Hanggi, P., Jung, P., and Marchesoni, F. (1998). Stochastic resonance. *Rev. Mod. Phys.*, **70**, p. 223.

Gao, J.B., Hwang, S.K., and Liu, J.M. (1999). When can noise induce chaos? *Phys. Rev. Lett.*, **82**, p. 1132.

Gassmann, F. (1997). Noise-induced chaos-order transitions. *Phys. Rev. E*, **55**, p. 2215.

Grasman, R.P.P.P., van der Maas, H.L.J., and Wagenmakers, E.-J. (2009). Fitting the cusp catastrophe in R: A cusp-package primer. *Journal of Statistical Software*, **32**, pp. 1–28.

Grubov, V.V., Hramov, A.E., Koronovskii, A.A., Kurovskaya, M.K., Pisarchik, A.N., and Runnova, A.E. (2017). Decision-making model and experimental study of the influence of stochastic processes on cognitive brain ability. *Phys. Lett. A* (submitted).

Horsthemke, W. and Lefever, R. (1984). *Noise-Induced Transitions*. Springer. Berlin.

Huguet, G., Rinzel, J., and Hupé, J. M. (2014). Noise and adaptation in multistable perception: Noise drives when to switch, adaptation determines percept choice. *Journal of Vision*, **14**, p. 19.

Lai, Y.C. and Grebogi, C. (1995). Intermingled basins and two-state on-off intermittency. *Phys. Rev. E*, **52**, p. R3313.

Lai, Y.C. and Tel, T. (2011). *Transient Chaos: Complex Dynamics on Finite Time Scales*. Springer. Berlin.

Matsumoto, K. and Tsuda, I. (1983). Noise-induced order. *J. Stat. Phys*, **31**, pp. 87–106.

McDonnell, M.D., Stocks, N.G., Pearce, C.E.M., and Abbott, D. (2008). *Stochastic Resonance: From Suprathreshold Stochastic Resonance to Stochastic Signal Quantization*. Cambridge University Press. Cambridge.

Moreno-Bote, R., Rinzel, J., and Rubin, N. (2007). Noise-induced alternations in an attractor network model of perceptual bistability. *J. Neurophysiol.*, **98**, pp. 1125–1139.

Moss, F. and McClintock, P.V.E. (1989). *Noise in Nonlinear Dynamical Systems*. Cambridge University Press, Cambridge.

Pikovsky, A.S. and Kurths, J. (1997). Coherence resonance in a noise-driven excitable system. *Phys. Rev. Lett.*, **78**, p. 775.

Pisarchik, A.N., Jaimes-Reátegui, R., Sevilla-Escoboza, R., and Huerta-Cuellar, G. (2012). Multistate intermittency and extreme pulses in a fiber laser. *Phys. Rev. E*, **86**, p. 056219.

Pisarchik, A.N., Jaimes-Reátegui, R., Magallón-García, C.D.A., and Castillo-Morales, C.O. (2014). Critical slowing down and noise-induced intermittency in bistable perception: bifurcation analysis. *Biol. Cybern.*, **108**, pp. 397–404.

Pisarchik, A.N., Bashkirtseva, I., and Ryashko, L. (2015). Controlling bistability in a stochastic perception model. *Eur. Phys. J. Spec. Topics*, **224**, pp. 1477–1484.

Ploeger, A., van der Maas, H.L.J., and Hartelman, P.A.I. (2002). Stochastic catastrophe analysis of switches in the perception of apparent motion. *Psychonomic Bulletin and Review*, **9**, pp. 26–42.

Poston, T. and Stewart, I. N. (1978). Nonlinear modeling of multistable perception. *Behavioral Science*, **23**, pp. 318–334.

Saunders, P.T. (1980). *Introduction to Catastrophe Theory*. Cambridge University Press. Cambridge.

Sevilla-Escoboza, R., Pisarchik, A.N., Jaimes-Reátegui, R., and Huerta-Cuellar, G. (2015). Selective monostability in multi-stable systems. *Proc. Roy. Soc. A*, **471**, p. 20150005.

Stewart, I. N. and Peregoy, P. L. (1983). Catastrophe theory modeling in psychology. *Psychological Bulletin*, **94**, pp. 336–362.

Ta'eed, L. K., Ta'eed, O., and Wright, J. E. (1988). Determinants involved in the perception of the Necker cube: An application of catastrophe theory. *Behavioral Science*, **33**, pp. 97–115.

Zeeman, C. (1977). *Catastrophe Theory: Selected Papers, 1972-77*. Addison-Wesley. Boston.

Appendix. Stochastic Sensitivity of Equilibrium

Consider a generic one-dimensional stochastic system:

$$\dot{x} = f(x) + \varepsilon\sigma(x)\xi(t), \quad (3)$$

where $\xi(t)$ is white Gaussian noise with parameters $\mathrm{E}(\xi(t)) = 0$, $\mathrm{E}(\xi(t)\xi(\tau)) = \delta(t-\tau)$ and ε is the noise intensity. Let $\bar{x}$ be a stable equilibrium of the system in Eq. (3) for $\varepsilon = 0$.

For small noise, we can write the following Gaussian approximation for probability density $\rho(x)$ of stationary distributed random states of the system in Eq. (3): $\rho(x) \approx k \cdot \exp\left[-\frac{(x-\bar{x})^2}{2D}\right]$, where $\bar{x}$ is the mean value and D is the dispersion.

The dispersion D can be represented as $D = \varepsilon^2 M$. Here, coefficient M connecting the value D of stochastic output with the value ε^2 of the stochastic input are given as $M = -\frac{\sigma^2(\bar{x})}{2f'(\bar{x})}$. The value M is the stochastic sensitivity function [Bashkirtseva and Ryashko, 2011] of equilibrium $\bar{x}$ for the system in Eq. (3).

Using the stochastic sensitivity M, one can find a confidence interval $(\bar{x} - r, \bar{x} + r)$. Stationary distributed random states of the system in Eq. ((3) belong to this confidence interval with fiducial probability $\mathcal{P}$. For the standard 3σ-rule with fiducial probability $\mathcal{P} = 0.997$, the parameter r of the confidence interval has a simple explicit representation $r = 3\varepsilon\sqrt{M}$.